

Characterizing the dark state in thymine and uracil by double resonant spectroscopy and quantum computation.

M. Ligare^a, F. Siouri^a, Ota Bludsky^b, D. Nachtigallova^{b*}, M.S. de Vries^{a*}.

a. Department of Chemistry and Biochemistry. University of California, Santa Barbara, CA 93117-9510. USA.

b. Institute of Organic Chemistry and Biochemistry v.v.i., AS CR, Flemingovo nam. 2, 16610 Prague, Czech Republic

Supporting Information Placeholder

ABSTRACT: We report on gas phase double resonant spectroscopy of the dark excited state in isolated uracil and thymine. In combination with ab initio calculations the results suggest that the dark state is of triplet ($^3\pi\pi^*$) character.

The ultra-short excited state lifetimes of isolated nucleic acid bases are a well-known phenomenon which was observed experimentally by several authors, both in the gas phase and in solution [1-4]. The primary mechanism is subpicosecond internal conversion to the electronic ground state. This process protects the nucleobases from otherwise potentially harmful UV-photochemistry. This property may have played a selective role in prebiotic chemistry on an early earth, considering that many non-canonical derivatives have long excited state lifetimes and that the intrinsic properties of the nucleobases must have been unchanged since their incorporation in the reproductive machinery. It is thus conceivable that the choice of the genetic alphabet was aided by a photochemical selection that preceded any biological evolution. If that is the case, the photochemical properties of the bases are molecular fossils of prebiotic chemistry. However for uracil and thymine the electronic relaxation pathway competes with another, poorly understood, process which causes a very small fraction of excited molecules to populate a “dark” excited state. Here we report on gas phase spectroscopy of that dark excited state in isolated uracil and thymine, which in combination with ab initio calculations suggests that the dark state is of triplet ($^3\pi\pi^*$) character.

Computational studies show that the rapid relaxation of photoexcited nucleobases to the ground state proceeds through nonadiabatic transitions via conical intersections on the crossing seam of potential energy surfaces of excited and ground states characterized by strongly ring-puckered structures [5-25]. Several conical intersections were found for naturally occurring nucleobases for which efficiencies depend on the reaction paths from the excited state minima to a particular structure on the crossing seam. A comprehensive study performed by Barbatti et. al. shows that the purine bases, guanine and adenine, relax with a single-exponential

decay along one excited state potential energy surface (PES) leading directly to the intersection with the ground state PES[26]. However, the pyrimidine-based nucleobases, cytosine, thymine and uracil, exhibit a more complex picture with several excited states involved in the relaxation process. A small portion of excited state molecules appears to populate a “dark state”, the character of which is unknown and which has been extensively debated in recent literature. As a result, the UV damage resistance is not complete and the dark state may act as a precursor to formation of photolesions by dimerization of adjacent pyrimidine bases in DNA. For thymine which has the longest excited-state lifetime among the nucleobases, photodynamics simulations show that after excitation to the S_2 state of $\pi\pi^*$ character the system relaxes to the minimum of the S_2 state. Due to the flat character of the PES of this state, the relaxation is delayed. S_2/S_1 intersections then lead to the S_1 state of $\pi\pi^*$ character where the system is trapped and an additional delay occurs before internal conversion to the ground state. This entire deactivation mechanism still proceeds on a picosecond timescale. However, an additional sub-nanosecond to nanosecond relaxation pathway to a non-fluorescent (“dark”) state has been reported in many experimental studies [1, 27] [28][1,2,3,4]. This state was also observed for methylated derivatives of uracil and thymine [29, 30].

Several candidates for the dark state have been suggested, including the vibrationally “hot” ground state, the S_1 state of $^1(n\pi^*)$ character, and the T_1 state of $^3(\pi\pi^*)$ or $^3(n\pi^*)$ character[27-33]. The involvement of different tautomeric forms of thymine was ruled out by Schultz and co-workers on the basis of theoretical calculations [28]. According to the current understanding of the photophysics of thymine, the $^3(\pi\pi^*)$ state is the most likely candidate. Three possible pathways have been suggested to populate this state from the initially excited $^1(\pi\pi^*)$ state: a direct $^1(\pi\pi^*) \rightarrow ^3(\pi\pi^*)$ path or one of two indirect pathways: $^1(\pi\pi^*) \rightarrow ^3(n\pi^*) \rightarrow ^3(\pi\pi^*)$ or $^1(\pi\pi^*) \rightarrow ^1(n\pi^*) \rightarrow ^3(\pi\pi^*)$ [31].

Several authors have interpreted time-resolved pump-probe ionization and vibrational spectra (ref 6-9,12) using excited state calculations are based mainly on characteriza-

tion of the potential energy surface and the spin-orbit coupling terms [30-32]. Etinski et al. [32] provided support of the triplet state based on the interpretation of time resolved infrared spectra in solution[33], in particular the peak at 1500 cm^{-1} , resulting from a combination of the C₄-C₅ stretching and the N₁H wagging motions, and the peak near 1350 cm^{-1} due to the ring deformation vibration.

In this work we propose an assignment of the long-lived dark state, based on NH vibrational frequencies of the dark state, obtained with double resonant IR-UV spectroscopy of excited state uracil and thymine. We interpret these frequencies using computational studies which include analysis of NH frequencies accounting for the anharmonicity effects.

The instrument has been previously described in detail [34]. A brief description of the instrument and experimental setup follows. Samples are placed on a translating graphite substrate directly in front of a pulsed molecular beam valve. They are laser desorbed by a Nd:YAG laser (1064nm, ~1 mJ/cm²), then entrained in a supersonic molecular beam of argon (6 atm backing pressure). The cold, neutral molecules are ionized by resonance enhanced multiphoton ionization (REMPI) and are subsequently detected by a reflectron time of flight mass spectrometer. For REMPI spectroscopy two lasers are spatially and temporally overlapped. The first and resonant photon comes from the frequency doubled output of a tunable dye laser (lumonics HD-300) with maximum spectral line width 0.4 cm^{-1} and pulse energy 0.3-0.7 mJ. The second photon comes from an excimer laser (193 nm, 1.5-2 mJ/pulse). A variable delay between dye laser and excimer laser allows measurement of excited state lifetimes. For IR-UV double resonance spectroscopy we use an additional IR laser in different pulse sequences, depending on whether the ground state or the dark state is probed, shown in Fig. 1 and detailed below [35-38]. The IR laser is an OPO/OPA (Laser Vision) pumped by a Nd:YAG laser (Quanta Ray DCR-2A, 550 mJ/pulse). The near-IR output has a pulse energy of 3-5 mJ over the range of 3200-3800 cm^{-1} and spectral width of 3 cm^{-1} . The standards for thymine and uracil were purchased from Sigma Aldrich and used without further purification.

The minimal structure, harmonic and anharmonic frequencies of the ground and excited states were calculated at the Moller-Plesset perturbation theory (MP2) [39] level and with the second-order algebraic diagrammatic construction (ADC(2)) method [40, 41], with the resolution of identity [42], respectively. The cc-pVTZ basis set [43] was used throughout the calculations. Anharmonic frequency calculations at the second-order perturbation theory (PT2) level were carried out for the ground electronic state using Gaussian09 [44]. One-dimensional NH stretching frequencies (1D-scan) were obtained by solving (1) using the Numerov-Cooley integration technique [45].

$$\left\{ -\frac{\hbar^2}{2\mu} \frac{d^2}{dr_{NH}^2} + V(r_{NH}) \right\} \chi_n(r_{NH}) = E_n \chi_n(r_{NH}), \quad (1)$$

where $\frac{1}{\mu} = \frac{1}{m_N} + \frac{1}{m_H}$ and $V(r_{NH})$ is a potential energy surface scan over the N-H bond coordinate. Assuming small coupling of the NH stretching motion with other vibrational degrees of freedom, the 1D-scan results should be compara-

ble to one-dimensional anharmonic frequencies evaluated from diagonal anharmonic constants (denoted as 1D-PT₂).

Both U and T have broad onsets in the UV, as first reported by Brady et al. [46]. We have now obtained higher resolution two photon spectra of U and T, showing the same onset as reported before, but now also showing some structure (Figure SF1 in supplemental information)

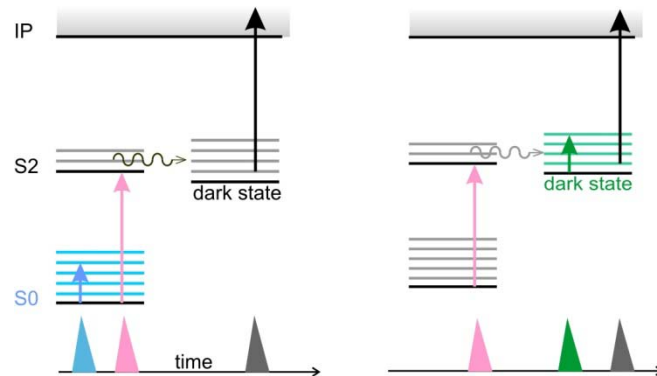


Figure 1: Pulse sequences employed to obtain ground state IR (left) and excited state IR (right panel).

We have obtained the first IR spectra of both uracil (Fig. 2) and thymine (Fig. 3) both for the ground state and for the dark state. The pulse sequences employed to obtain these spectra appear in Figure 1. For the ground state, an initial IR pulse is scanned in the NH and OH stretch frequency region and followed by two step ionization probing. When the IR pulse is resonant with a vibrational frequency this modifies the ground state vibrational population producing a modified Franck-Condon landscape. Usually this reduces the ion probe signal, but in this case it increases the ion probe signal. This suggests a strong geometry change between S₀ and S₂, which would also be consistent with the gradual onset of the UV absorption.

For the dark state the pulse sequence starts with excitation to S₂ (purple pulse) followed by rapid relaxation to the dark state. After 20 ns the IR laser is fired (green pulse) followed after another 30 ns by the ionization pulse from the excimer laser (black pulse), serving as the probe. In this sequence the IR laser modifies the dark state vibrational population, producing the green ion-dip spectra.

We have obtained lifetimes for the dark state by nanosecond pump probe measurements. We achieve this by varying the delay between the excitation laser pulse and the ionization laser pulse (purple and black in Figure 1). For uracil the lifetime varies from 59 to 69 ns, depending on wavelength. For thymine the lifetime is longer and depends more strongly on excitation wavelength, increasing with excitation energy from 248 ns at 36,364 cm^{-1} to 293 ns at 37,015 cm^{-1} . We postulate that this wavelength dependence reflects the de-excitation dynamics for which analysis is currently being undertaken. For thymine we also observe a very long time-scale component, with a lifetime longer than our experimental window of eight microseconds. We interpret this signal as due to ionization out of the hot ground state, resulting from the rapid internal conversion out of the $\pi\pi^*$ state.

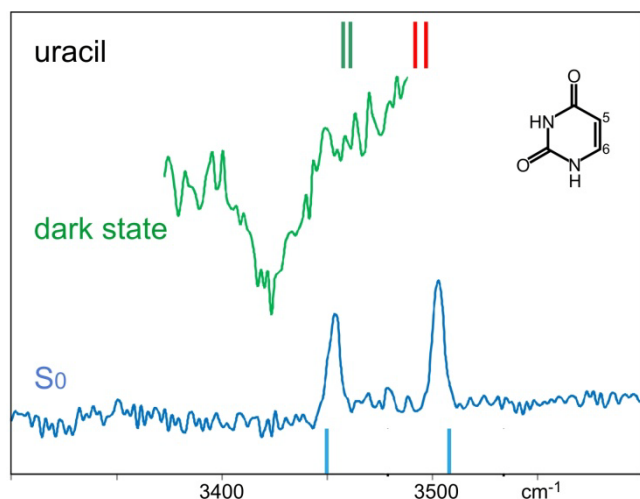


Figure 2: IR-UV double resonant spectra of the ground state (blue) and dark excited state of uracil (green). Computed frequencies of the NH stretches are indicated as stick spectra. The frequencies of S_0 state (blue) are obtained with fully-dimensional anharmonic calculations. The S_1 (red) and T_1 (green) frequencies are estimated from the 1D-scan with the assumption of the same corrections for full anharmonicity as for the S_0 state.

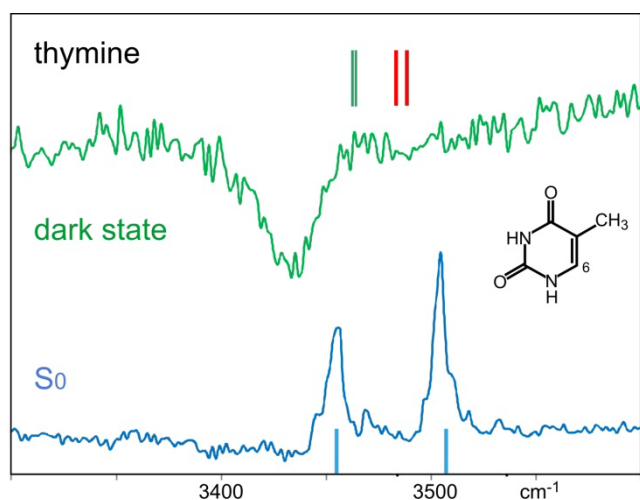


Figure 3: Same data as in Figure 2 for thymine.

In agreement with previously reported studies on thymine and uracil, the minima of the S_1 states of both species are of $n \rightarrow \pi^*$ character with almost planar structure, similar to the ground state minima. The minima of S_2 are characterized by a distortion from planarity with pyramidalization at the C6 atom [10, 47-50].

The triplet state minima are of $\pi \rightarrow \pi^*$ character and they are also characterized by pyramidalization of the pyrimidine ring at the C6 atom. The calculated NH stretching frequencies in the ground state and excited state of thymine and uracil appear in Tables S1 and S2, respectively. We evaluated the anharmonic effects for the NH stretching mode for the ground state, both by employing one-dimensional scans of the NH bond length (1D-scan) and from the diagonal anharmonic constants corresponding to NH stretching modes (1D-PT2).

For both systems the former method gives slightly smaller corrections compared to the 1D-PT2 calculations. The differences are, however, small and justify the reliability of 1D-scan calculations. Both methods yield a blue-shift of about 30 cm^{-1} with respect to the experimentally observed frequencies which are recovered in fully-dimensional anharmonic PT2 calculations. Comparison of the results of PT2 with both 1D-PT2 and 1D-scan indicate a relatively small coupling between NH stretching modes and other degrees of freedom. In addition, these calculations which accounted for full-dimensional anharmonicity provided frequencies in a very good agreement with the experiment, confirming that this is the diketo tautomer as seen in previous experiments [51-56]. The frequencies appear as blue stick spectra in Figures 2 and 3.

The resulting NH vibrational frequencies for S_1 are nearly degenerate with a splitting of 5 cm^{-1} for both species. The frequencies obtained with 1D-scan corrections show blue shifts of 29 and 34 cm^{-1} and 35 and 40 cm^{-1} with respect to the lower-energy frequency of the ground states of thymine and uracil, respectively, shown in red in Figs 2 and 3. The structural dynamics, represented by a complex behavior of vibrations at the S_1 and S_0 minima, is expected to be very similar due to their structural similarities. Consequently, the effects of anharmonicity are expected to be similar and, thus, the full-dimensional anharmonic calculations are expected to give very similar effects for S_1 and S_0 . Based on these assumptions the frequencies corresponding to the S_1 state are predicted to fall into the region of $3480\text{-}3490 \text{ cm}^{-1}$, i.e. blue-shifted from the lower NH stretching band by about $30 - 40 \text{ cm}^{-1}$.

As in the case of the S_1 minima, the calculations performed for the T_1 minima predict only small splittings of the NH frequencies of 1 and 3 cm^{-1} for thymine and uracil, respectively. The calculated shifts with respect to the lower-energy NH frequency of the ground states are significantly smaller than for the S_1 state, at 8 and 9 cm^{-1} and 2 and 5 cm^{-1} for thymine and uracil, respectively (in green in Figs. 2 and 3). Importantly, these structures are energetically separated from their corresponding global minima by 3.65 and 2.69 kcal/mol in the case of thymine and uracil, respectively.

The prediction of the position of the NH stretching band of the S_1 state, made with the assumption of similar effects of anharmonicity as calculated for the S_0 state, indicate that the observed spectra of both species correspond more likely to the T_1 rather than S_1 states. Contrary to the S_1 state, more complex behavior is expected for the T_1 state where the distorted global minimum structures are separated by small barriers (see above) from the planar structures.

These barriers could be responsible for the discrepancy between the experimentally observed and calculated spectral shifts between the S_0 and T_1 states. In particular, the assumption of the same corrections for fully-dimensional anharmonicity as used for S_0 and S_1 states predicts blue shifts of about 9 and 5 cm^{-1} for thymine and uracil, respectively, while we observe small red-shifts of about 10 (thymine) and 20 (uracil) cm^{-1} experimentally. Due to the complexity of the vibrational dynamics in T_1 states, the low energy vibrations are expected to further influence the coupling with NH stretching modes. A more detailed study of this coupling is in progress.

Supporting Information

Table ST1. Vibrational frequencies of the NH stretching modes of thymine. Table ST2. Vibrational frequencies of the NH stretching modes of uracil. Figure SF1 R2PI spectra.

AUTHOR INFORMATION

Corresponding Authors

devries@chem.ucsb.edu,
dana.nachtigallova@uochb.cas.cz.

ACKNOWLEDGMENT

This material is based upon work supported by the National Science Foundation under CHE-1301305 and by NASA under Grant No. NNX12AG77. D.N. acknowledges the funding of the Grant Agency of the Czech Republic (P208/12/1318). The research at IOCB was a part of the project RVO:61388963.

REFERENCES

- [1] H. Kang, K.T. Lee, B. Jung, Y.J. Ko, S.K. Kim, *J. Am. Chem. Soc.*, 124 (2002) 12958-12959.
- [2] S. Ullrich, T. Schultz, M.Z. Zgierski, A. Stolow, *PCCP*, 6 (2004) 2796-2801.
- [3] C. Canuel, M. Mons, F. Piuze, B. Tardivel, I. Dimicoli, M. Elhanine, *J. Chem. Phys.*, 122 (2005).
- [4] P.M. Hare, C.E. Crespo-Hernandez, B. Kohler, *Proceedings of the National Academy of Sciences of the United States of America*, 104 (2007) 435-440.
- [5] H.R. Hudock, B.G. Levine, A.L. Thompson, H. Satzger, D. Townsend, N. Gador, S. Ullrich, A. Stolow, T.J. Martinez, *J. Phys. Chem. A*, 111 (2007) 8500.
- [6] H. Chen, S.H. Li, *J. Chem. Phys.*, 124 (2006).
- [7] S. Perun, A.L. Sobolewski, W. Domcke, *J. Phys. Chem. A*, 110 (2006) 13238.
- [8] S. Perun, A.L. Sobolewski, W. Domcke, *J. Am. Chem. Soc.*, 127 (2005) 6257-6265.
- [9] L. Serrano-Andres, M. Merchán, A.C. Borin, *Proceedings of the National Academy of Sciences of the United States of America*, 103 (2006) 8691-8696.
- [10] S. Matsika, *J. Phys. Chem. A*, 108 (2004) 7584-7590.
- [11] N. Ismail, L. Blancafort, M. Olivucci, B. Kohler, M.A. Robb, *J. Am. Chem. Soc.*, 124 (2002) 6818-6819.
- [12] A.L. Sobolewski, W. Domcke, *European Physical Journal D*, 20 (2002) 369-374.
- [13] E. Epifanovsky, K. Kowalski, P.D. Fan, M. Valiev, S. Matsika, A.I. Krylov, *J. Phys. Chem. A*, 112 (2008) 9983-9992.
- [14] L. Serrano-Andres, M. Merchán, A.C. Borin, *J. Am. Chem. Soc.*, 130 (2008) 2473-2484.
- [15] S. Perun, A.L. Sobolewski, W. Domcke, *Chem. Phys.*, 313 (2005) 107-112.
- [16] M. Barbatti, H. Lischka, *J. Am. Chem. Soc.*, 130 (2008) 6831.
- [17] E. Fabiano, W. Thiel, *J. Phys. Chem. A*, 112 (2008) 6859-6863.
- [18] C.M. Marian, *J. Phys. Chem. A*, 111 (2007) 1545-1553.
- [19] Z.G. Lan, E. Fabiano, W. Thiel, *ChemPhysChem*, 10 (2009) 1225-1229.
- [20] M. Barbatti, J.J. Szymczak, A.J.A. Aquino, D. Nachtigallova, H. Lischka, *J. Chem. Phys.*, 134 (2011) 014304.
- [21] M. Barbatti, A.J.A. Aquino, J.J. Szymczak, D. Nachtigallova, H. Lischka, *PCCP*, 13 (2011) 6145-6155.
- [22] K.A. Kistler, S. Matsika, *J. Chem. Phys.*, 128 (2008) 215102-215114.
- [23] L. Blancafort, M.A. Robb, *J. Phys. Chem. A*, 108 (2004) 10609-10614.
- [24] A.L. Sobolewski, W. Domcke, *PCCP*, 6 (2004) 2763-2771.
- [25] M.Z. Zgierski, S. Patchkovskii, T. Fujiwara, E.C. Lim, *J. Phys. Chem. A*, 109 (2005) 9384-9387.
- [26] M. Barbatti, A.J.A. Aquino, J.J. Szymczak, D. Nachtigallova, P. Hobza, H. Lischka, *Proceedings of the National Academy of Sciences of the United States of America*, 107 (2010) 21453-21458.
- [27] Y.G. He, C.Y. Wu, W. Kong, *J. Phys. Chem. A*, 107 (2003) 5145-5148.
- [28] J. Gonzalez-Vazquez, L. Gonzalez, E. Samoylova, T. Schultz, *Phys. Chem. Chem. Phys.*, 11 (2009) 3927-3934.
- [29] M. Kunitski, Y. Nosenko, B. Brutschy, *ChemPhysChem*, 12 (2011) 2024-2030.
- [30] M. Busker, M. Nispel, T. Häber, K. Kleinermanns, M. Etinski, T. Fleig, *ChemPhysChem*, 9 (2008) 1570-1577.
- [31] J.J. Serrano-Perez, R. Gonzalez-Luque, M. Merchán, L. Serrano-Andres, *J. Phys. Chem. B*, 111 (2007) 11880-11883.
- [32] M. Etinski, T. Fleig, C.A. Marian, *J. Phys. Chem. A*, 113 (2009) 11809-11816.
- [33] P.M. Hare, C.T. Middleton, K.I. Mertel, J.M. Herbert, B. Kohler, *Chem. Phys.*, 347 (2008) 383-392.
- [34] G. Meijer, M.S. Devries, H.E. Hunziker, H.R. Wendt, *Applied Physics B-Photophysics and Laser Chemistry*, 51 (1990) 395-403.
- [35] T. Ebata, C. Minejima, N. Mikami, *J. Phys. Chem. A*, 106 (2002) 11070-11074.
- [36] B.C. Dian, A. Longarte, T.S. Zwier, *J. Chem. Phys.*, 118 (2003) 2696-2706.
- [37] T. Ebata, N. Mizuochi, T. Watanabe, N. Mikami, *J. Phys. Chem.*, 100 (1996) 546-550.
- [38] T. Walther, H. Bitto, T.K. Minton, J.R. Huber, *Chem. Phys. Lett.*, 231 (1994) 64-69.
- [39] C. Moller, M.S. Plesset, *Phys Rev*, 46 (1934) 618-622.
- [40] C. Hattig, *Advances in Quantum Chemistry*, Vol 50, 50 (2005) 37-60.
- [41] A. Kohn, C. Hattig, *J. Chem. Phys.*, 119 (2003) 5021-5036.
- [42] C. Hattig, *J. Chem. Phys.*, 118 (2003) 7751-7761.
- [43] T.H. Dunning, *J. Chem. Phys.*, 90 (1989) 1007-1023.
- [44] V. Barone, *J. Chem. Phys.*, 122 (2005).
- [45] J.W. Cooley, *Math Comput*, 15 (1961) 363.
- [46] B.B. Brady, L.A. Peteanu, D.H. Levy, *Chem. Phys. Lett.*, 147 (1988) 538-543.
- [47] J.J. Szymczak, M. Barbatti, J.T.S. Hoo, J.A. Adkins, T.L. Windus, D. Nachtigallova, H. Lischka, *J. Phys. Chem. A*, 113 (2009) 12686-12693.
- [48] H.R. Hudock, B.G. Levine, A.L. Thompson, H. Satzger, D. Townsend, N. Gador, S. Ullrich, A. Stolow, T.J. Martinez, *J. Phys. Chem. A*, 111 (2007) 8500-8508.
- [49] Z.G. Lan, E. Fabiano, W. Thiel, *J. Phys. Chem. B*, 113 (2009) 3548-3555.
- [50] D. Nachtigallova, A.J.A. Aquino, J.J. Szymczak, M. Barbatti, P. Hobza, H. Lischka, *J. Phys. Chem. A*, 115 (2011) 5247-5255.
- [51] V. Vaquero, M.E. Sanz, J.C. Lopez, J.L. Alonso, *J. Phys. Chem. A*, 111 (2007) 3443-3445.
- [52] R.N. Casaes, J.B. Paul, R.P. McLaughlin, R.J. Saykally, T. van Mourik, *J. Phys. Chem. A*, 108 (2004) 10989-10996.
- [53] M.R. Viant, R.S. Fellers, R.P. McLaughlin, R.J. Saykally, *J. Chem. Phys.*, 103 (1995) 9502-9505.
- [54] C. Puzzarini, M. Biczysko, V. Barone, I. Pena, C. Cabezas, J.L. Alonso, *PCCP*, 15 (2013) 16965-16975.
- [55] J.C. Lopez, J.L. Alonso, I. Pena, V. Vaquero, *PCCP*, 12 (2010) 14128-14134.
- [56] J.C. Lopez, M.I. Pena, M.E. Sanz, J.L. Alonso, *J. Chem. Phys.*, 126 (2007).

TOC GRAPHIC:

